# Alteration of Nonlinear Refraction by Mixing Clusters $[WOS_3Cu_3I(py)_5]$ and $[MoOS_3Cu_3I(py)_5]$

**P. Ge, S. H. Tang, and W. Ji***

*Physics Department, National University of Singapore, Singapore 119260, Republic of Singapore*

**S. Shi**

*SS-ALL Technologies, Singapore 079903, Republic of Singapore*

**H. W. Hou, D. L. Long, and X. Q. Xin**

*Chemistry Department, Nanjing University, Nanjing 210008, People's Republic of China*

**S. F. Lu and Q. J. Wu**

*State Key Laboratory of Structural Chemistry, Fujian Institute of Research on Structure of Matter, Chinese Academy of Sciences, Fuzhou 350002, People's Republic of China*

*Received: June 20, 1996*[⊗]

A new cluster compound $[WOS_3Cu_3I(py)_5]$ **(I)** was synthesized by substitution reactions of $(Et_4N)_3[WOS_3Cu_3I_4]$ with pyridine and structurally determined by X-ray diffraction. It crystallizes in monoclinic, space group *C*2/*c* (No. 15), $a = 24.341(1)$, $b = 10.020(4)$, $c = 26.64(1)$ Å, $V = 6424(3)$ Å$^3$, and $Z = 8$. The cluster has a nest-shaped skeleton. The nonlinear optical properties of both **I** and $[MoOS_3Cu_3I(py)_5]$ **(II)** in acetonitrile solutions were measured using a Z-scan technique with 7-ns and 532-nm laser pulses. Compound **I** possesses a self-focusing property ($n_2 = 1.6 \times 10^{-9}$ cm$^2$ W$^{-1}$ M$^{-1}$), while compound **II** exhibits a self-defocusing property ($n_2 = -1.3 \times 10^{-10}$ cm$^2$ W$^{-1}$ M$^{-1}$). Both compounds show reverse saturable absorption ($\alpha_2 = 1.5 \times 10^{-4}$ and $2.5 \times 10^{-5}$ cm W$^{-1}$ M$^{-1}$ for compounds **I** and **II**, respectively). We demonstrate that the nonlinear refraction of a mixture containing the two compounds can be altered from self-focusing, through a state where self-lensing disappears, to self-defocusing by varying the ratio of the two compounds.

## 1. Introduction

In recent years, reverse saturable absorption (RSA) has attracted attention because of its potential in optical limiting and optical pulse shaping. RSA occurs in a nonlinear optical (NLO) material when its excited-state absorption cross section is larger than its ground-state absorption cross section. RSA has been observed in a number of molecules including fullerenes,[1,2] phthalocyanines,[3,4] and metal clusters.[5−10] As incident light energy increases, these molecules are excited to the excited state, which results in stronger absorption. Such RSA may be applied to optical limiting for protecting optical sensors from damages induced by intense laser radiation. In the cases of fullerenes,[2] phthalocyanines,[4] and some metal clusters,[5−8] the excited state involved is a long-lived state. As a result, the RSA is an accumulative process, which can be exploited for shortening optical pulses. If the excited state has a much shorter lifetime, as compared to the excitation duration, then the RSA is effectively an irradiance-dependent absorption process,[10] which can be used for reduction of laser amplitude fluctuations, i.e., pulse smoothing.

It has been observed that many RSA materials also possess nonlinear refractive properties, particularly under high irradiances of incident light.[3,9,10] The presence of refractive nonlinearities may be used to enhance the optical-limiting performance if a focusing geometry is employed and an on-axis aperture is positioned in front of the optical sensor. However, the occurrence of the nonlinear refraction can also distort the transmitted light beam. The beam distortion imposes serious problems in the device design for optical-limiting and pulse-shaping applications. For example, in a hybrid optical limiter using a RSA material and a two-photon-absorption self-defocusing semiconductor,[11] the semiconductor is normally placed at a focus of the device as a primary limiter. Because such a semiconductor has a relatively low photodamage threshold, a more photostable RSA material is inserted as a protection layer in front of the semiconductor. Problems may arise if the RSA molecule possesses a self-lensing property. The self-lensing effect changes the focal point of the device, resulting in the degradation of the semiconductor limiting performance. If the RSA molecule exhibits a self-focusing property, the insertion of the RSA material may induce damage on the semiconductor, which is the opposite of what a protection layer is supposed to do.

In this article we present a method to alter the nonlinear refraction by using a mixture of two soluble NLO materials with mutually opposite self-lensing effects. This is demonstrated here with two RSA cluster compounds: $[WOS_3Cu_3I(py)_5]$ **(I)** and $[MoOS_3Cu_3I(py)_5]$ **(II)**. These two clusters have been synthesized by substitution reactions. We also report our investigation on the molecular structure of compound **I**. The molecular structure of compound **II** was published before.[12] The two compounds have similar nest-shaped structures but different signs of nonlinear refraction. The Z-scan measurements show that compound **I** possesses a strong self-focusing efect, while compound **II** exhibits a self-defocusing effect. The mixture of the two compounds is stable in acetonitrile solutions. This offers a practically very simple way to tune the nonlinear refraction.

* To whom the correspondence should be addressed.

⊗ Abstract published in *Advance ACS Abstracts,* December 1, 1996.

S1089-5647(96)01837-8 CCC: $14.00 

By varying the molecular ratio of the two compounds, the refractive nonlinearity of the mixture can be changed from self-focusing, through a state where no self-lensing occurs, to self-defocusing. This tunability may be applied, for example, to eliminate self-lensing effects of RSA molecules used as an element in devices for optical-limiting and pulse-shaping applications.

## 2. Experiment

**2.1. Synthesis.** $(NH_4)_2WO_2S_2$ was prepared according to literature.[13] $[MoOS_3Cu_3I(py)_5]$ was synthesized using the method described elsewhere.[12] The other chemicals were purchased as A.R. grade reagents and used without further purification.

*$(Et_4N)_3[WOS_3Cu_3I_4]$*. A well-ground mixture of $(NH_4)_2WO_2S_2$ (0.32 g, 1 mmol), CuI (0.38 g, 2 mmol), and $Et_4NI$ (0.51 g, 2 mmol) was placed in a reaction tube and heated at 95 °C for 10 h under a pure nitrogen atmosphere. Extraction of the product with $CH_2Cl_2$ (20 mL) and the subrequest filtration produced a yellow clear solution. Dropwise addition of 2-propanol (10 mL) to the top of the solution produced a two-layer system from which orange-yellow crystals (0.11 g) were obtained after standing for 5 days. Infrared (IR) spectra of the crystals were recorded on a Fourier Nicolet FT-170SX spectrophotometer with pressed KBr pellets. The crystals show characteristic IR absorption at 911 $cm^{-1}$ (W−$O_t$) and 432 $cm^{-1}$ (W−$S_b$). Carbon, hydrogen, and nitrogen analyses were performed on a PE 240C elemental analyzer. Anal. Calcd for $C_{24}H_{60}N_3Cu_3I_4OS_3W$: C, 20.80; H, 4.33; N, 3.03. Found: C, 21.22; H, 4.45; N, 3.08.

*$[WOS_3Cu_3I(py)_5]$*. $(Et_4N)_3[WOS_3Cu_3I_4]$ (0.10 g) was dissolved in pyridine (20 mL). After stirring for 1 h, the yellow solution was filtered and 2-propanol (10 mL) was added dropwise to the top of the solution. Yellow crystals (0.09 g) were produced a few days later. Characteristic IR absorption was observed at 928 $cm^{-1}$ (W−$O_t$) and 431 $cm^{-1}$ (W−$S_b$). Anal. Calcd for $C_{25}H_{25}N_5Cu_3WIOS$: C, 29.75; H, 2.48; N, 6.94. Found: C, 29.50; H, 2.67; N, 6.54.

**2.2. Crystal Data and Structure Determination.** Suitable crystals of compound $[WOS_3Cu_3I(py)_5]$ were mounted in random orientation on a glass fiber. Data were collected on a diffractometer using Mo Kα radiation at 296 K. Details concerning the intensity and data collection are given in Table 1. The data were corrected for Lorentz and polarization factors, and absorption was corrected for by using empirical scan data and DIFABS. The structure of the compound was determined by direct methods. The structure was refined by full-matrix least-squares fits with isotropic temperature factors for C atoms and anisotropic temperature factors for the remaining non-hydrogen atoms to final $R = 0.044$ and $R_w = 0.052$. All calculations were carried out on an MICRO-VAX II computer with a TEXSAN program package (TEXSAN-TEXRAY Structure Analysis Package, Molecular Structure Corp., 1985). The atomic coordinations and thermal parameters are summarized in Table 2.

**2.3. Nonlinear Optical Measurements.** All the optical measurements were conducted at room temperature with compounds $[WOS_3Cu_3I(py)_5]$ and $[MoOS_3Cu_3I(py)_5]$ dissolved in acetonitrile ($CH_3CN$) and contained in 1-mm-thick quartz cuvettes. The ultraviolet (UV) and visible spectra of the compounds in solutions were taken with a Shimadzu UV-240 or a Hitachi U3410 spectrophotometer. The Z-scan[14] measurements were carried out with a Q-switched, frequency-doubled Nd:YAG laser, which produced linearly polarized, 7-ns (FWHM), 532-nm optical pulses. The spatial profiles of the laser pulses were nearly Gaussian after passing through a spatial filter. The laser beam was divided by a beam splitter into two parts. The reflected part was taken as a reference representing the incident light energy; and the transmitted beam was focused through

**TABLE 1: Crystallographic Data for $[WOS_3Cu_3I(Py)_5]$**

| | |
|---|---|
| chemical formula | $WICu_3S_3ON_5C_{25}H_{25}$ |
| formula weight | 1009.08 |
| color | yellow |
| crystal system | monoclinic |
| space group | *C*2/*c* (No. 15) |
| unit-cell parameters | |
| *a* (Å) | 24.341(4) |
| *b* (Å) | 10.020(4) |
| *c* (Å) | 26.64(1) |
| $\beta$ (deg) | 98.56(2) |
| *V* (Å$^3$) | 6424(3) |
| *Z* | 8 |
| $\mu$ ($cm^{-1}$) | 67.81 |
| *F*(000) | 3840 |
| $2\theta$ (deg) | 49.9 |
| *h*, *k*, *l* ranges | 0→29, −11→0, −31→31 |
| $d_{calc}$ ($g/cm^3$) | 2.09 |
| temperature (K) | 296 |
| diffractometer | Enraf-nonius CAD4 |
| radiation (Å) | Mo Kα ($\lambda$ 0.710 69) |
| solution method | direct methods |
| absorption correction | empirical |
| residuals: *R*; $R_w$ | 0.044; 0.052 |
| no. of unique data | 6031 |
| no. obs. with $I > 3\sigma(I)$ | 4088 |
| no. of variables | 352 |
| max shift in final cycle | 0.03 |
| largest peaks in final diff map | 0.74 |

**TABLE 2: Positional Parameters and *B*(eq)**

| atom | *x* | *y* | *z* | *B*(eq) |
|---|---|---|---|---|
| W | 0.303 062 | 0.415 473 | 0.176 931 | 3.512 |
| I | 0.399 494 | 0.258 076 | 0.044 903 | 5.064 |
| Cu(1) | 0.362 105 | 0.446 51 | 0.098 784 | 3.875 |
| Cu(2) | 0.362 966 | 0.601 11 | 0.232 225 | 4.386 |
| Cu(3) | 0.230 306 | 0.601 91 | 0.137 705 | 4.686 |
| S(1) | 0.396 51 | 0.439 42 | 0.184 61 | 4.21 |
| S(2) | 0.266 71 | 0.433 62 | 0.094 41 | 4.11 |
| S(3) | 0.268(61) | 0.579 53 | 0.220 61 | 4.61 |
| O | 0.286 74 | 0.264 27 | 0.200 43 | 6.54 |
| N(1) | 0.385 64 | 0.620 57 | 0.066 63 | 3.94 |
| N(2) | 0.390 64 | 0.791 18 | 0.225 53 | 4.54 |
| N(3) | 0.395 34 | 0.574 58 | 0.308 73 | 4.64 |
| N(4) | 0.233 63 | 0.793 47 | 0.108 03 | 4.04 |
| N(5) | 0.143 54 | 0.578 1 | 0.125 14 | 5.55 |
| C(11) | 0.417 05 | 0.624 1 | 0.029 14 | 4.85 |
| C(12) | 0.432 76 | 0.740 1 | 0.008 24 | 5.96 |
| C(13) | 0.416 46 | 0.858 1 | 0.025 55 | 6.47 |
| C(14) | 0.383 56 | 0.858 1 | 0.063 35 | 6.27 |
| C(15) | 0.370 15 | 0.739 1 | 0.083 74 | 5.05 |
| C(21) | 0.362 25 | 0.895 1 | 0.241 45 | 5.76 |
| C(22) | 0.374 57 | 1.024 1 | 0.235 57 | 7.89 |
| C(23) | 0.419 1 | 1.053 2 | 0.211 88 | 121 |
| C(24) | 0.451 1 | 0.948 2 | 0.197 08 | 121 |
| C(25) | 0.432 77 | 0.818 1 | 0.204 25 | 7.18 |
| C(31) | 0.365 25 | 0.608 1 | 0.345 45 | 5.86 |
| C(32) | 0.386 77 | 0.606 2 | 0.394 94 | 7.38 |
| C(33) | 0.441 37 | 0.572 2 | 0.409 54 | 7.78 |
| C(34) | 0.472 66 | 0.529 1 | 0.373 35 | 7.17 |
| C(35) | 0.446 95 | 0.534 1 | 0.323 34 | 5.66 |
| C(41) | 0.254 85 | 0.893 1 | 0.136 84 | 5.66 |
| C(42) | 0.263 77 | 1.017 1 | 0.116 36 | 7.38 |
| C(43) | 0.250 16 | 1.037 1 | 0.064 96 | 7.07 |
| C(44) | 0.226 86 | 0.936 1 | 0.037 15 | 6.57 |
| C(45) | 0.218 66 | 0.815 1 | 0.059 25 | 5.86 |
| C(51) | 0.119 76 | 0.472 1 | 0.100 75 | 6.57 |
| C(52) | 0.063 87 | 0.454 2 | 0.089 66 | 8.09 |
| C(53) | 0.031 06 | 0.554 2 | 0.103 06 | 8.19 |
| C(54) | 0.053 67 | 0.664 2 | 0.128 96 | 7.58 |
| C(55) | 0.111 07 | 0.672 1 | 0.137 76 | 7.78 |

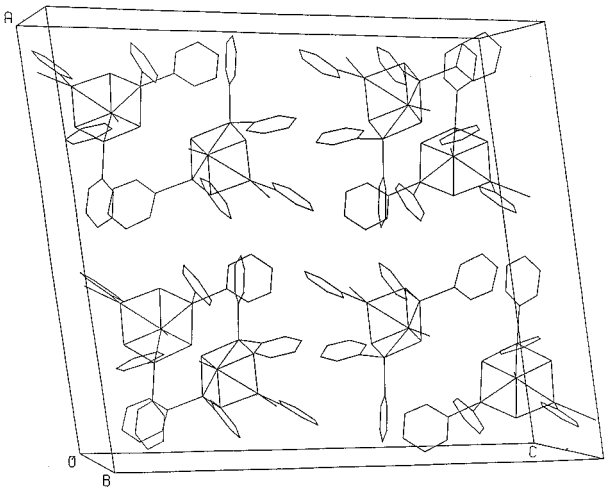


**Figure 1.** ORTEP diagram of $[WOS_3Cu_3I(py)_5]$.

the sample. The spot radius of the laser pulses at the focus was measured to be of $30 \pm 5$ $\mu$m (half-width of $1/e^2$ maximum in irradiance). Both the incident and transmitted pulse energies were monitored simultaneously by using two energy detectors (Laser Precision, RjP-735 energy probes). The detectors were linked to a computer by an IEEE interface. The sample was mounted on a translation stage which was controlled by the computer to adjust the sample position along the *Z* axis with respect to the focal point. To avoid any effect from possible photochemical degradation, the interval between the two sequential laser pulses used in all the measurements was set at 20 s so that the experiments were effectively single shots on fresh molecules. To measure the nonlinear refraction, an on-axis aperture ($S = 0.06$) was placed in front of the transmission detector. To test the apparatus, we measured the third-order refractive nonlinearity ($n_2$) of $CS_2$. A value of $(5 \pm 2) \times 10^{-14}$ cm$^2$/W or $(2.0 \pm 0.8) \times 10^{-11}$ esu was obtained for $n_2$ in $CS_2$, which is in good agreement with the reported value of $1.2 \times 10^{-11}$ esu.[14] We also conducted similar measurements on $CH_3CN$ to assess the solvent contribution to the observed nonlinearities described in the following section. The nearly flat lines in the *Z* scans confirmed that the solvent played an insignificant role under our experimental conditions.

## 3. Results and Discussion

**3.1. Description of the Structure of Compound $[WOS_3Cu_3I(py)_5]$ (I).** The skeleton of **I**, consisting of one W atom, three $\mu_3$-S atoms, and three Cu atoms, assumes a nest-shaped structure similar to that of $[MoOS_3Cu_3X(py)_5]$ (X = Br, I) reported before.[12] The ORTEP diagram and cell packing of **I** are given in Figures 1 and 2. The W atom is tetrahedrally coordinated by three S atoms and one terminal O atom. The W−O bond length of 1.709(7) is typical for an Mo═O double bond. The three W−S bond lengths fall in the range of W−S single bonds. One of the three Cu atoms is coordinated by the I atom, two $\mu_3$-S atoms, and an N atom of a pyridine. Each of the other two Cu atoms binds to two $\mu_3$-S atoms and two N atoms of other two pyridines. All of the three Cu atoms adopt distorted tetrahedral geometry. Selected bond lengths and bond angles of **I** are listed in Tables 3 and 4 in comparison with those of **II** reported in ref 12. The structures of **I** and **II** are very similar. The W═O, average W−S, W−Cu, and S−Cu bond lengths in **I** are 1.709(7), 2.255(3), 2.688(2), and 2.294(3) Å, while the Mo═O, average Mo−S, Mo−Cu, and S−Cu bond lengths in **II** are 1.70(1), 2.274(5), 2.682(3), and 2.285(5) Å. The average O−W−S, S−W−S, and Cu−W−Cu angles in **I** are 110.1(3), 108.9(1), and 91.06(5)°, while the O−Mo−S, S−Mo−S, and Cu−Mo−Cu angles in **II** are 110.7(5), 108.2(2), and 90.47(8)°.

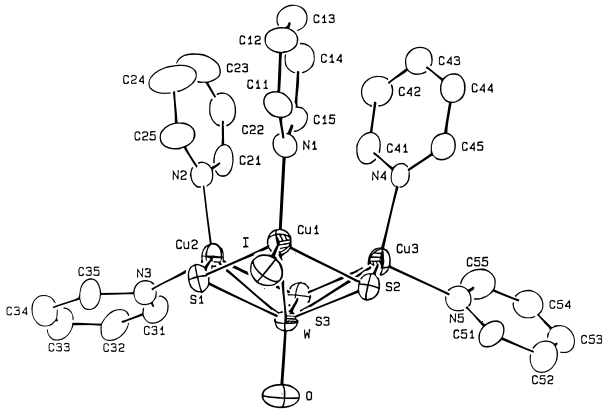


**Figure 2.** Cell packing of $[WOS_3Cu_3I(py)_5]$.

**TABLE 3: Selected Bond Lengths (Å) for $[WOS_3Cu_3I(py)_5]$**

| | | | |
|---|---|---|---|
| W−Cu(1) | 2.718(1) | W−Cu(2) | 2.667(2) |
| W−S(1) | 2.247(3) | W−Cu(3) | 2.678(2) |
| W−O | 1.709(7) | W−S(2) | 2.252(3) |
| Cu(1)−S(2) | 2.312(3) | W−S(3) | 2.265(3) |
| Cu(2)−N(3) | 2.089(8) | Cu(1)−N(1) | 2.062(7) |
| Cu(3)−N(4) | 2.082(8) | Cu(1)−N(2) | 2.035(9) |
| Cu(3)−S(2) | 2.294(3) | Cu(2)−S(3) | 2.283(3) |
| I−Cu(1) | 2.615(2) | Cu(3)−S(3) | 2.276(3) |
| Cu(2)−S(1) | 2.282(3) | Cu(1)−S(1) | 2.315(3) |
| Cu(3)−N(5) | 2.100(1) | | |

**TABLE 4: Selected Bond Angles (deg) for $[WOS_3Cu_3I(py)_5]$**

| | | | |
|---|---|---|---|
| Cu(3)−W−Cu(2) | 90.25(5) | Cu(2)−W−Cu(1) | 92.02(5) |
| Cu(3)−W−Cu(1) | 90.90(5) | O−W−S(3) | 109.5(3) |
| O−W−S(2) | 110.5(3) | O−W−S(1) | 110.2(3) |
| S(3)−W−S(2) | 108.8(1) | S(3)−W−S(1) | 108.9(1) |
| S(2)−W−S(1) | 108.9(1) | N(1)−Cu(1)−I | 104.0(2) |
| N(1)−Cu(1)−W | 128.8(2) | S(2)−Cu(1)−S(1) | 105.1(1) |
| I−Cu(1)−W | 127.20(5) | N(2)−Cu(2)−N(3) | 97.1(3) |
| N(2)−Cu(2)−W | 139.9(2) | S(1)−Cu(2)−S(3) | 107.1(1) |
| N(3)−Cu(2)−W | 123.0(2) | N(4)−Cu(3)−N(5) | 98.0(3) |
| N(4)−Cu(3)−W | 137.0(2) | S(3)−Cu(3)−S(2) | 106.4(1) |
| N(5)−Cu(3)−W | 124.9(2) | | |

**3.2. Nonlinear Optical Properties.** The UV−visible absorption spectra of $[WOS_3Cu_3I(py)_5]$ and $[MoOS_3Cu_3I(py)_5]$ in acetonitrile are displayed in Figure 3. It is noticed that the two compounds have relatively low linear absorption at wavelengths ranging from 600 to 1000 nm. The spectrum of a mixture of the two compounds is simply a superposition of the individual spectra of the two compounds. No chemical reaction is observed between the compounds in the $CH_3CN$ solvent. The optical properties of the mixture is hence expected to be a simple sum of the those of the individual compounds.

Figure 4 shows typical *Z*-scan measurements of the individual compounds in acetonitrile with and without the aperture. The open circles are the data measured without the aperture. They clearly illustrate that the absorption increases as the incident light irradiance arises, which is the characteristics of RSA process. Note that the normalized transmittance of compound **I** or **II** drops to about 80% at the focus where the peak irradiance is a few hundreds of MW/cm$^2$ (or fluence $\sim$ a few J/cm$^2$). This performance is comparable to the limiting behavior observed in $C_{60}$, which has been widely investigated as one of the best optical limiting materials.[1,2] The origin of the observed RSA in compound **I** or **II** can be attributed to excited-state absorption. We have performed time-resolved nonlinear transmission studies on $(n\text{-}Bu_4N)_4[Mo_8Cu_{12}O_8S_{24}]$, a mixed metal cluster that has a

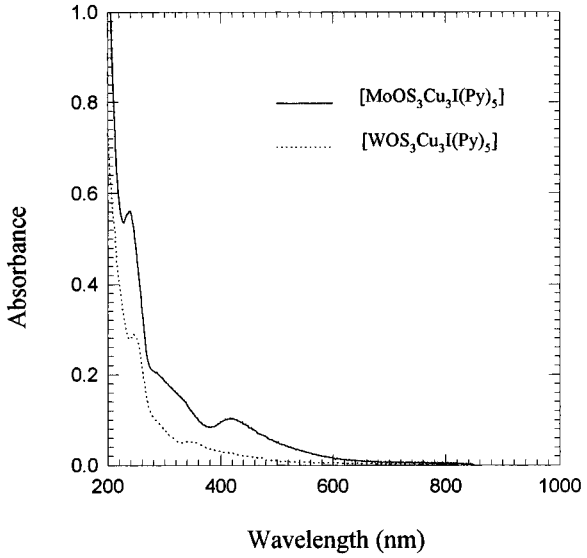


**Figure 3.** Absorption spectra of $[WOS_3Cu_3I(py)_5]$ and $[MoOS_3Cu_3I(py)_5]$ in acetonitrile solution with 1-mm optical path. The $[WOS_3Cu_3I(py)_5]$ and $[MoOS_3Cu_3I(py)_5]$ concentrations are $1.4 \times 10^{-4}$ and $2.3 \times 10^{-3}$ M, respectively.

similar nest-shaped structure, and the results revealed that the triplet−triplet transitions should be a responsible mechanism.[9,15]

The filled circles in Figure 4 are the *Z*-scan data measured with the aperture, and they indicate that the two compounds have opposite signs of refractive nonlinearity. The data in Figure 4a show that compound **I** has a positive sign for the refractive nonlinearity, which gives rise to self-focusing. The data in Figure 4b indicate that compound **II** has a self-defocusing property. We have performed a series of *Z* scans on the compounds over a range of incident peak irradiances, from 25 to 800 MW/cm$^2$. The measurements confirm that the observed NLO effects are effectively third order in nature, which implies that both the absorption coefficient and refractive index should be expressed as $\alpha = \alpha_0 + \alpha_2 I$ and $n = n_0 + n_2 I$, respectively, where $\alpha_0$ and $\alpha_2$ are the linear and nonlinear absorption coefficient; $n_0$ and $n_2$ are the linear and nonlinear refractive index, respectively; and $I$ is the irradiance of the light. By applying the *Z*-scan theory,[14] the solid curves in Figure 4 are numerically calculated to fit to the experimental data. The best fits reveal that $\alpha_2 = 1.5 \times 10^{-4}$ cm W$^{-1}$ M$^{-1}$, $n_2 = 1.6 \times 10^{-9}$ cm$^2$ W$^{-1}$ M$^{-1}$ for compound **I**; and $\alpha_2 = 2.5 \times 10^{-5}$ cm W$^{-1}$ M$^{-1}$, $n_2 = -1.3 \times 10^{-10}$ cm$^2$ W$^{-1}$ M$^{-1}$ for compound **II**.

Recently, Sheik-Bahae et al.[16] have developed a two-band model to predict the dispersion of third-order refractive nonlinearity due to bound electronic effects for a spectral region below the fundamental absorption edge of a material. Their model shows that sign of $n_2$ is positive when the photon energy is smaller than $0.7E_g$, where $E_g$ is the bandgap energy of the material. The nonlinear refraction becomes negative when the photon energy is in the range from $0.7E_g$ to $E_g$. These theoretical predictions are in agreement with observation in many wide-gap dielectrices and semiconductors. We compare this theory with our results. Table 5 lists the measured signs and values of compounds **I**, **II**, and other metal clusters that we studied before.[9,10,15−20] It is evident that the measured signs of $n_2$ in all the clusters are consistent with the theory if the bandgap energy is replaced by the position of the lowest absorption peak ($\hbar\omega_0$). Although compounds **I** and **II** have similar structures, replacing atom W for Mo results in a red-shift for the lowest absorption band, as shown in Figure 3, due to the heavy-atom effect. Consequently, the nonlinear refraction

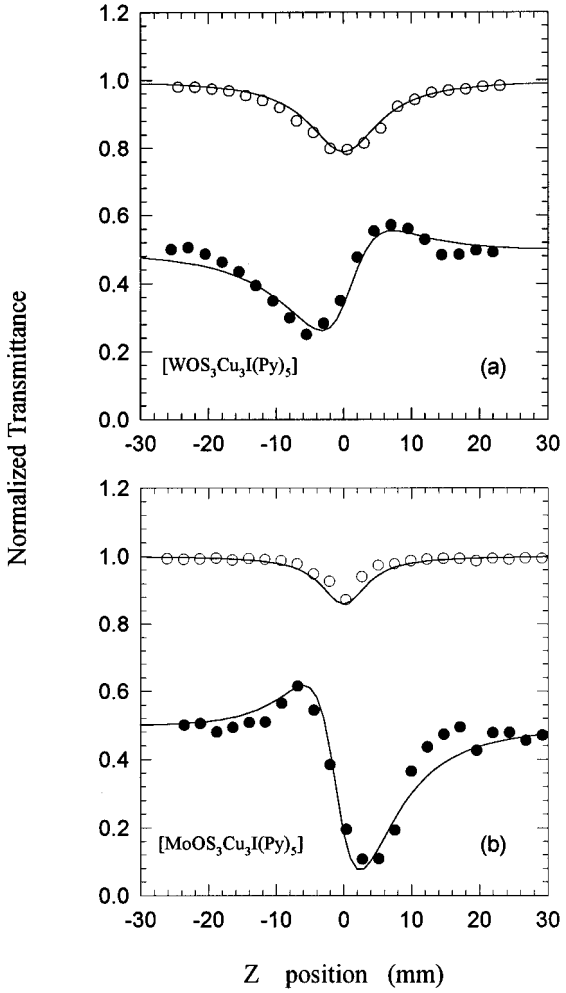


**Figure 4.** *Z*-scan measurements at 532 nm. The filled and open circles are the data measured with and without the aperture, respectively. The data in (a) are obtained with $[WOS_3Cu_3I(py)_5]$ at a concentration of $1.7 \times 10^{-4}$ M and a peak irradiance of $3.7 \times 10^8$ W/cm$^2$. The data in (b) are obtained with $[MoOS_3Cu_3I(py)_5]$ at a concentration of $2.6 \times 10^{-3}$ M and a peak irradiance of $6.7 \times 10^8$ W/cm$^2$. The solid curves are the theoretical fits by using the *Z*-scan theory described in ref 14. The data (and corresponding fits) obtained with the aperture are vertically shifted by −0.5 for presentation.

**TABLE 5: Nonlinear Refraction in Mixed Metal Clusters at Photon Energy $\hbar\omega = 2.33$ eV**

| materials | $\hbar\omega_0$ (eV) | $\hbar\omega/\hbar\omega_0$ | $n_2$ ($10^{-10}$ cm$^2$ W$^{-1}$ M$^{-1}$) | ref |
|---|---|---|---|---|
| $(Me_4N)_2[Cu_4(SPH)_6]$ | 4.95 | 0.47 | 50 | 17 |
| $WCu_2OS_3(PPh_3)_4$ | 4.85 | 0.48 | 6.7 | 18 |
| $MoCu_2OS_3(PPh_3)_3$ | 4.80 | 0.49 | 68 | 18 |
| $Mo_2Ag_4S_8(PPh_3)_4$ | 4.75 | 0.49 | 120 | 10 |
| $(NEt_4)_3[WOS_3(CuBr)_3(\mu_2\text{-Br})]\cdot 2H_2O$ | 3.55 | 0.66 | 12 | 19 |
| $WOS_3Cu_3I(py)_5$ | 3.50 | 0.67 | 16 | this work |
| $MoOS_3Cu_3I(py)_5$ | 2.95 | 0.79 | −1.3 | this work |
| $(n\text{-}Bu_4N)_2[MoCu_3OS_3(NCS)_3]$ | 2.50 | 0.93 | −1.7 | 20 |
| $(n\text{-}Bu_4N)_4[Mo_8Cu_{12}O_8S_{24}]$ | 2.43 | 0.96 | −23 | 9, 15 |

is switched from self-focusing to self-defocusing by the model of Sheik-Bahae et al.

This switch is very useful in many applications since it enables one to alter the nonlinear refraction by using a mixture of the two compounds. To demonstrate this alteration, we conducted *Z* scans on mixtures of the two compounds. The experimental results and their fits are shown in Figure 5. By decreasing the $[WOS_3Cu_3I(py)_5]$ concentration and increasing the $[MoOS_3Cu_3I(py)_5]$ concentration, the overall nonlinear refractive index is tuned from positive to negative while the

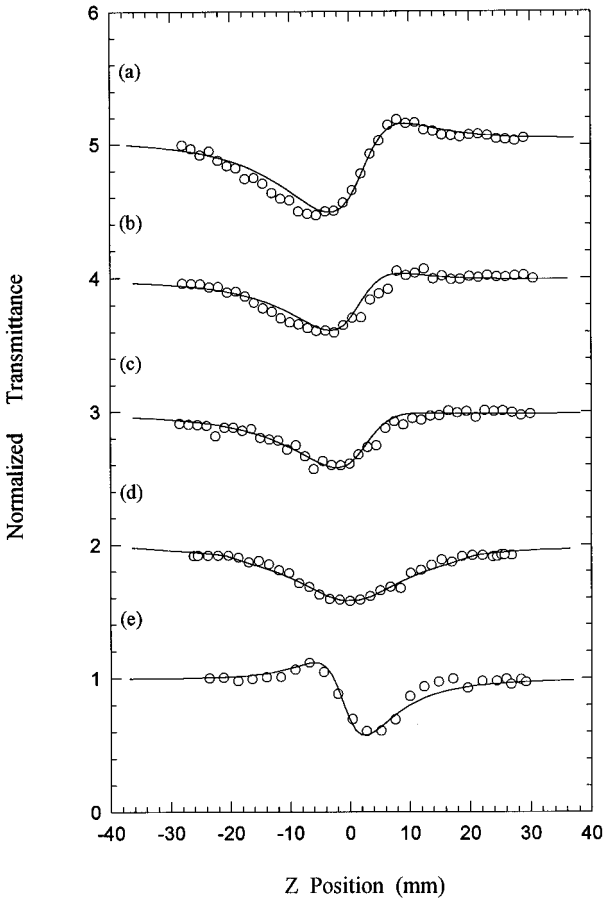


**Figure 5.** *Z*-scan data measured with the aperture at 532 nm and a peak irradiance of $6.5 \times 10^8$ W/cm$^2$. The circles are the results obtained with mixtures of $[WOS_3Cu_3I(py)_5]$ and $[MoOS_3Cu_3I(py)_5]$ at ratios of the two molecule concentrations: (a) 1:0; (b) 1:7; (c) 1:11; (d) 1:14; (e) 0:1. The solid curves are the theoretical fits by using the theory in ref 14. The circles and curves in (a), (b), (c), and (d) are vertically shifted by 4, 3, 2, and 1, respectively, for presentation.

nonlinear absorption remains almost unchanged. Figure 5d shows that within our experimental error, no self-lensing is observed when the concentration ratio of **I:II** is 1:14. This tunability is important in designing optical-limiting devices and optical elements for pulse-shaping applications. It can provide one with a practical method to control self-lensing effects in device fabrication.

## 4. Summary

We have presented two RSA clusters $[WOS_3Cu_3I(py)_5]$ and $[MoOS_3Cu_3I(py)_5]$. These two compounds possess similar molecular structures but have opposite effects in their nonlinear refractive properties, which provides an effective way to alter the nonlinear refraction by using a mixture of the two compounds.

**Supporting Information Available:** Description of X-ray diffraction data collection and refinement procedures, cell parameters, tables of atomic coordinates, bond distances, bond angles, anisotropic displacement parameters, along with all of the corresponding standard deviations, table of least-squares planes, dihedral angles and standard deviations (12 pages). Ordering information is given on any current masterhead page.

## References and Notes

(1) Tutt, L. W.; Kost, A. *Nature* **1992**, *356*, 225.
(2) McLean, D. G.; Sutherland, R. L.; Brant, M. C.; Brandelik, D. M.; Fleitz, P. A.; Pottenger, T. *Opt. Lett.* **1993**, *18*, 858.
(3) Wei, T. H.; Hagan, D. J.; Sence, M. J.; Van Stryland, E. W.; Perry, J. W.; Coulter, D. R. *Appl. Phys. B* **1992**, *54*, 46.
(4) Perry, J. W.; Mansour, K.; Marder, S. R.; Perry, K. J.; Alvarez Jr., D.; Choong, L. *Opt. Lett.* **1994**, *19*, 525.
(5) Tutt, L. W.; McCahon, S. W. *Opt. Lett.* **1990**, *15*, 700.
(6) Shi, S.; Ji, W.; Lang, J. P.; Xin, X. Q. *J. Phys. Chem.* **1994**, *98*, 3570.
(7) Shi, S.; Ji, W.; Tang, S. H.; Lang, J. P.; Xin, X. Q. *J. Am. Chem. Soc.* **1994**, *116*, 3615.
(8) Ji, W.; Du, H. J.; Tang, S. H.; Shi, S. *J. Opt. Soc. Am.* **1995**, *12*, 876.
(9) Shi, S.; Ji, W.; Xin, X. Q. *J. Phys. Chem.* **1995**, *99*, 894.
(10) Ji, W.; Shi, S.; Du, H. J.; Ge, P.; Tang, S. H.; Xin, X. Q. *J. Phys. Chem.* **1995**, *99*, 17297.
(11) Hagan, D. J.; Xia, T.; Said, A. A.; Wei, T. H.; Van Stryland, E. W. *Intl. J. Nonlinear Opt. Phys.* **1993**, *2*, 483.
(12) Hou, H. W.; Xin, X. Q.; Luo, S. F.; Huang, X. Y.; Wu, Q. J. *J. Coord. Chem.* **1995**, *35*, 225.
(13) McDonald, J. W.; Friesen, G. D.; Rosenhein, L. D.; Newton, W. E. *Inorg. Chim. Acta* **1983**, *72*, 205.
(14) Sheik-Bahae, B.; Said, A. A.; Wei, T. H.; Hagan, D. J.; Van Stryland, E. W. *IEEE J. Quantum Electron.* **1990**, *26*, 760.
(15) Ji, W.; Xie, W.; Tang, S. H.; Shi, S. *Mater. Chem. Phys.* **1996**, *43*, 45.
(16) (a) Sheik-Bahae, M.; Hagan, D. J.; Van Stryland, E. W. *Phys. Rev. Lett.* **1990**, *65*, 96. (b) Sheik-Bahae, M.; Hutching, D. C.; Hagan, D. J.; Van Stryland, E. W. *IEEE J. Quantum Electron.* **1991**, *27*, 1296.
(17) Shi, S.; Zhang, X.; Shi, X. F. *J. Phys. Chem.* **1995**, *99*, 14911.
(18) Shi, S.; Hou, H. W.; Xin, X. Q. *J. Phys. Chem.* **1995**, *99*, 4050.
(19) Chen, Z. R.; Hou, H. W.; Xin, X. Q.; Yu, K. B.; Shi, S. *J. Phys. Chem.* **1995**, *99*, 8717.
(20) Shi, S.; Ji, W.; Xie, W.; Chong, T. C.; Zeng, H. C.; Lang, J. P.; Xin, X. Q. *Mater. Chem. Phys.* **1995**, *39*, 298.